Published in final edited form as:
Neuroimage. 2011 October 15; 58(4): 1121–1130. doi:10.1016/j.neuroimage.2011.06.085.

visual one？？？

Heterogeneity of Functional Activation During Memory Encoding Across Hippocampal Subfields in Temporal Lobe Epilepsy

Sandhitsu R. Das[a], **Dawn Mechanic-Hamilton**[b], **John Pluta**[a,b], **Marc Korczykowski**[b], **John A. Detre**[b], and **Paul A. Yushkevich**[a]

Sandhitsu R. Das: sudas@seas.upenn.edu

[a]Penn Image Computing and Science Laboratory (PICSL), Department of Radiology, University of Pennsylvania

[b]Center for Functional Neuroimaging, Department of Neurology, University of Pennsylvania

Abstract

Pathology studies have shown that the anatomical subregions of the hippocampal formation are differentially affected in various neurological disorders, including temporal lobe epilepsy (TLE). Analysis of structure and function within these subregions using magnetic resonance imaging (MRI) has the potential to generate insights on disease associations as well as normative brain function. In this study, an atlas-based normalization method (Yushkevich et al., 2009) was used to label hippocampal subregions, making it possible to examine subfield-level functional activation during an episodic memory task in two different cohorts of healthy controls and subjects diagnosed with intractable unilateral TLE. We report, for the first time, functional activation patterns within hippocampal subfields in TLE. We detected group differences in subfield activation between patients and controls as well as inter-hemispheric activation asymmetry within subfields in patients, with dentate gyrus (DG) and the anterior hippocampus region showing the greatest effects. DG was also found to be more active than CA1 in controls, but not in patients' epileptogenic side. These preliminary results will encourage further research on the utility of subfield-based biomarkers in TLE.

偶发/片段的
难处理的
有病灶的那一侧

Keywords

hippocampus; shape-based normalization; postmortem atlas; fMRI; interhemispheric asymmetry; subfields; temporal lobe epilepsy

1 Introduction

Temporal lobe epilepsy (TLE) is a common neurological disorder in which seizures arise from the hippocampus. Approximately 30% of patients with TLE are refractory to medical therapy and are candidates for resective surgery as the only remaining treatment option (Engel, 1996). Although temporal lobectomy has been shown to provide highly significant benefits from the perspective of seizure reduction or elimination, it can be complicated by memory deficits, since the hippocampus normally plays a critical role in memory consolidation (Squire, 1992) and retrieval (Nadel and Moscovitch, 1997). Accordingly, pre-

surgical evaluation for temporal lobectomy includes both seizure lateralization and attempts to assess the functional integrity of the hippocampus that will be resected.

Structural and functional abnormalities in the epileptogenic hippocampi in patients have been documented in TLE using MRI for more than a decade (Lencz et al., 1992; Bookheimer, 1996; Bellgowan et al., 1998). Functional activation in the hippocampus has been shown to predict post-surgical seizure outcome (Killgore et al., 1999) as well as cognitive outcome (Rabin et al., 2004). Inter-hemispheric activation asymmetry in the hippocampus has also been used to lateralize memory function (Jokeit et al., 2001; Golby et al., 2002; Deblaere et al., 2005) during pre-surgical evaluation.

The hippocampus consists of anatomically distinct subregions, known as hippocampal subfields, that contain different neuronal cell types, and are connected with each other and with surrounding subcortical and cortical structures in the medial temporal lobe (MTL) in different ways. Accordingly, the hippocampal region is affected by various neurological disorders in a spatially non-uniform, complex fashion (Sass et al., 1991; Huesgen et al., 1993; Saravia et al., 2006). In a recent pioneering MRI-based volumetry study in a cohort of TLE patients, atrophy was found in dentate gyrus (DG) and CA3, and sometimes in CA1 and CA2 subfields (Mueller et al., 2009). This was the first attempt to segment and measure volumes of hippocampal subfields in TLE. The same group has also reported correlation of memory impairment with volume loss in subfields (Mueller et al., 2011). Recent histopathological studies have found plastic changes and abnormal sprouting of mossy fibers – which connect DG with CA3 – due to epileptogenic activity or neuron death (Andrade-Valença et al., 2008; McAuliffe et al., 2011). Therefore, focal measurements based on individual subfields may provide valuable insight about the disease process in TLE.

Most prior functional imaging studies in TLE have considered the hippocampus as a single region of interest (ROI). A few studies have segregated group effects into anterior and posterior regions (Bettus et al., 2009; Figueiredo et al., 2008; Das et al., 2009), but to our knowledge, none have examined functional activation patterns across hippocampal subfields. Subfield-based structural morphometry, however, has been shown to provide superior information than whole hippocampus based measurements (Mueller et al., 2009), correlated with performance in memory tasks (Mueller et al., 2011), and used to study other neurological disorders such as Alzheimer's disease (Mueller et al., 2008) and post-traumatic stress disorder (Wang et al., 2010). Further, in non-clinical populations, hippocampal subfields have been shown to exhibit dissociation of cognitive function (Zeineh et al., 2003; Bakker et al., 2008; Suthana et al., 2010; Duncan et al., 2011). Based on these findings, we hypothesize that analysis of functional activation within hippocampal subfields will augment existing knowledge on TLE pathology as well as normal memory function mediated by the hippocampus and can potentially be more sensitive to disease effects than whole hippocampus-based measurements.

There are a number of existing methods for analyzing functional activation in hippocampal subfields (Stark and Okado, 2003; Zeineh et al., 2003). These methods vary in the type of structural images used to label subfields or the labeling technique used, or both. A method used in Zeineh et al. (2003), and recently enhanced in Ekstrom et al. (2009), requires an initial manual segmentation of hippocampal gray matter, white matter and cerebrospinal fluid (CSF), in images with high in-plane resolution of 0.4×0.4 mm in slices oriented obliquely along the long axis of the hippocampus. It then uses a computational flattening technique that allows the gray matter sheet in MTL to be transformed into a flat space, where activations within subfields can be computed, and group-wise statistical analysis can be performed. The ROI-AL technique (Stark and Okado, 2003; Miller et al., 2005; Bakker et al., 2008) uses more common T1-weighted structural images with ≈1 mm isotropic

resolution, as we use in the present study, and uses image registration to an atlas containing subfield labels to segment ROIs in individual subjects. The atlas is constructed by manually segmenting subfield ROIs in *in vivo* images with 0.75 mm isotropic resolution from several subjects, and averaging the ROI labels in a common space after spatial normalization driven by the label images (Kirwan et al., 2007). In contrast, we use shape-based normalization to a high-resolution atlas (Yushkevich et al., 2009) that was constructed from *ex vivo* MRI scans of resolution 0.2×0.2×0.2 mm or 0.2×0.3×0.2 mm to label subfields in individual hippocampi. The benefit of this approach is that the subfields can be distinguished in the postmortem images reliably, with the tradeoff that no intensity information is used from the *in vivo* image, where subfields are difficult to distinguish (see section 2.3.3 for details). In our previous work, we have used shape-based normalization to establish voxel-by-voxel correspondence within the hippocampus (Yushkevich et al., 2007; Das et al., 2009) to perform group statistical analysis of activation maps, but this work did not include subfield ROI. In this study, we used subfield labels to determine functional activation within subfields in both healthy controls and patients with TLE. We then compared activations in different subfields across subject groups. We also studied inter-hemispheric activation asymmetry, a measure that is often used to lateralize pre-surgical cognitive function in TLE (Jokeit et al., 2001; Golby et al., 2002; Deblaere et al., 2005). We demonstrate both subfield-specific group differences in functional activation, and hemispheric differences in subfield activation within the same subject.

2 Materials and Methods

2.1 Image Acquisition

This paper analyzes data from two independent TLE studies. The first study, denoted TLE-HR, was designed with detailed hippocampal morphometry in mind and collected high-resolution fMRI data. An older study, denoted TLE-SR (for standard resolution), collected more routine 3mm isotropic fMRI data. MRI images were obtained from a 3T Siemens Trio scanner using a product T/R head coil and body coil transmitter. For both datasets, the imaging protocol consisted of a localizer scan, followed by an anatomical scan, and a functional MRI (fMRI) scan while the subjects performed a complex scene encoding task in a blocked design experiment. The T1-weighted anatomical scans used the MP-RAGE sequence with the following parameters: TR=1620 ms, TE=3.87 ms, TI=950 ms, flip angle=150, 160 sagittal slices, matrix size= 256×192 and voxel size = 0.9375×0.9375×1 mm^3. The BOLD fMRI scans used a gradient echo echoplanar (EPI) sequence with TR = 3000 ms, TE = 30 ms. The TLE-HR dataset used a resolution of 1.95×1.95×2 mm^3 (ip angle=90, 30 oblique slices, matrix size=128×128), did not cover the whole brain, but included the entire temporal lobe. The TLE-SR dataset used a 3×3×3 mm^3 (ip angle=90, 40 axial slices, matrix size=64×64) resolution and imaged the whole brain. Note that the former dataset – having higher spatial resolution that yielded voxels that are more than 3 times smaller than the latter – was more suitable for studies of BOLD activation in small hippocampal subfields. A resolution of 2 mm or lower is typically considered to be high-enough resolution (Carr et al., 2010) for such studies. As such, the TLE-HR dataset should be considered our primary dataset for the current study. Nonetheless, the motivation for presenting independent analyses on both datasets are twofold: 1) On the one hand, if broadly similar effects can be demonstrated in two disjoint cohorts, it serves as a validation of the results, 2) On the other hand, the way the results differ in the two datasets can also help interpret them, and inform us about the possible effects of spatial resolution. Also note that activation within some larger subfield ROIs may be distinguishable in the lower resolution TLE-SR dataset.

Experimental paradigm—In both datasets, alternating blocks consisted of a task condition when the subjects were instructed to remember visual scenes of people, landscape and human-created environments, and a control condition when they viewed randomly scrambled scenes. In the TLE-HR cohort, subjects also indicated whether the scene was meaningful to them in some way or not during the task condition, and performed a visual search task during the control condition where they had to locate an embedded "X" or "T" in the scrambled scene. Subjects indicated their binary choice for both conditions by a button press. Further details of the task can be found in Rabin et al. (2004).

2.2 Subjects

The TLE-HR dataset consisted of 15 patients with TLE and 19 healthy volunteers with no history of neurological illness. 8 patients had seizures originating in the left hemisphere and 5 on the right hemisphere. 2 had bilateral seizure foci. The TLE-SR dataset consisted of 18 patients with TLE and 19 healthy volunteers with no history of neurological illness. 9 patients had seizures originating in the left hemisphere and 7 on the right hemisphere. 2 had bilateral seizure foci. Patients with bilateral seizures were not included in the analysis. Structural and functional imaging data were obtained for the healthy volunteers in the same way as for the patients.

2.3 Image Processing

2.3.1 Whole hippocampus segmentation—Each subject's hippocampi were segmented using a semi-automated protocol (Pluta et al., 2009), in which a few user-defined landmarks are used to drive diffeomorphic normalization of the subject's MRI to a disease-specific template with manual whole-hippocampus segmentations. This produced a whole hippocampus label in the subject space that was edited by an expert. The initial landmark placement and final editing of the mask required 15 minutes on average for a trained rater. This procedure had an inter-rater reliability of 89.5% as measured by DICE overlap (Dice, 1945).

2.3.2 Postmortem hippocampus atlas—A computational atlas of the human hippocampus was used as described in Yushkevich et al. (2009). Briefly, *ex vivo* sections of the human medial temporal lobe are imaged in a 9.4T animal scanner at a resolution of 0.2×0.2×0.2 mm or 0.2×0.3×0.2 mm. At this resolution, the layer of tissue sometimes referred to as the *dark band* that separates the major cell layers of subfields CA and DG, is visible in MRI. Subregions of the CA subfield – CA1, CA2, and CA3 are segmented according to criteria described in Yushkevich et al. (2010). Head and tail regions, which can be thought of as separate labels for anterior and posterior regions of the hippocampus, were labeled as separate subregions. This was done to be able to compare our results with existing studies that use these regions as separate labels, as well as to be consistent with labeling schemes used in high resolution *in vivo* images (Mueller et al., 2009; Yushkevich et al., 2010). Part of the subiculum is included in the HEAD label, as well as in the CA1 label in the body region. The postmortem images are combined using shape and intensity averaging to create an atlas consisting of the hippocampal subfield labels (Fig. 1).

2.3.3 Labeling of subfields using shape-based normalization—Prior to shape-based normalization, the *in vivo* whole hippocampus segmentation image was resampled to a resolution of 0.195×0.195×0.2 mm that was roughly 5 times that of the original T1-weighted image, and similar to that of the postmortem atlas. Subfields of the hippocampal formation were then labeled in subjects' anatomical space using shape-based normalization of this resampled mask to the postmortem atlas. Note that the resampling does not improve the anatomical resolution of the *in vivo* image, but the segmentation mask has smoother boundary and helps generate smoother subfield masks after normalization. It also helps

reduce partial volume effects between subfield labels in the mapped segmentation. A continuous, invertible coordinate mapping was computed between the interior of each whole-hippocampus segmentation and the atlas. This mapping is derived from representing the hippocampus in subject space and in atlas space using a geometrical model known as the *continuous medial representation* (Yushkevich et al., 2006). The mapping approximately preserves the relative distances of points between the boundary of the hippocampus and the medial axis (skeleton) of the hippocampus; it also preserves the relative position of the points' projection onto the medial axis. This mapping is said to provide *shape-based normalization* (SBN) between the interiors of objects. The coordinate mapping produced by shape-based normalization makes it possible to propagate the subfield labels from atlas space into subject space, yielding a subfield segmentation in subject space (Fig. 1). This technique assumes that the shape of the whole hippocampus – as defined by the boundary of the whole hippocampus and represented by medial geometry – faithfully describes the relative locations of the subfields within the hippocampal volume. It also assumes that the effects of postmortem preservation of tissue on the relative positions of hippocampal subfields are relatively insignificant. The main advantage of SBN is that for regions where image intensity is homogeneous, the geometrical mapping behaves in a much more predictable way than image normalization, which in these regions is driven by very localized regularization priors, due to lack of strong consistent intensity features (Yushkevich et al., 2007; Sun et al., 2007). The accuracy of this labeling technique has been evaluated in postmortem data (Yushkevich et al., 2008), where even in the presence of intensity features that can distinguish subfields, image-based normalization performed only slightly better than SBN.

2.3.4 Region of interest analysis of fMRI data within labeled subfields—The functional data were motion corrected and realigned with the first EPI volume, and a mean EPI image was computed and co-registered to the structural MRI image, using Statistical Parametric Mapping (SPM5) software (Friston et al., 1995). The EPI time-series data were then resampled using linear interpolation to the high-resolution space of the hippocampus subfield segmentation. Specifically, resampling was performed by sampling intensity values from raw EPI volumes at locations computed by combining realignment and co-registration transformations computed by SPM. All further analyses were carried out in the high-resolution space of the hippocampus subfield segmentation. It has been shown that analyzing functional data in higher resolution anatomical space in this manner can help increase spatial specificity and reproducibility of measurements by effectively increasing the spatial resolution of the underlying data (Kang et al., 2007). No smoothing of the functional data was done to further enhance our ability to localize functional activation within subfields. This increases spatial specificity of our measurements at the cost of loss of some sensitivity (Yushkevich et al., 2007; Tabelow et al., 2008).

A general linear model (GLM) was then used to model the EPI signal as

$$Y_{ij}=f_j\beta_i+\mu_i+\varepsilon_i$$

where Y_{ij} is the EPI signal at time j and voxel i; f is the convolution of a boxcar function and a canonical model of the hemodynamic response function; and β_i, μ_i, and ε_i model the task effect, the constant offset in the EPI signal, and the noise, respectively, at voxel i. The noise was modeled as non-spherical and the parameters were estimated using the restricted maximum likelihood (ReML) approach (Friston et al., 2002). SPM5 was used to solve the GLM and generate task contrast images that were used for ROI based analysis. Fig. 2 shows an example of a task contrast map within the hippocampus of a subject. Subfield-specific

functional activation A_S in subfield S was measured by integrating all the positive task contrast values over a subfield label as

$$A_S = \sum_{\{i:\beta_i>0, i\in S\}} \beta_i$$

Hemispheric activation asymmetry AI_S (Golby et al., 2002) in subfield S was then measured as

$$AI_S = (A_{S_L} - A_{S_R})/(A_{S_L} + A_{S_R})$$

where A_{S_L} and A_{S_R} are activation in the left and right subfields respectively. Analysis used two sets of four ROI labels – each at different spatial scales. The first set included whole hippocampus (HIPP), and its three subregions along the longitudinal axis: HEAD, BODY and TAIL labels (coarse parcellation). The BODY region contained four subfield labels: CA1, CA2, CA3 and DG (fine parcellation). CA2 and CA3 were not included separately in the analysis as measurements within these very small ROIs are likely to be unreliable. Instead, we used the following four labels: CA1, DG, CA3DG (CA3+DG) and CA (CA1+CA2+CA3). CA3 was included in the CA3DG label, as has been done by other researchers (Bakker et al., 2008). The CA2 subfield was included in the CA label. Some of the subregions used in our analysis are morphologically defined as subfields (e.g. CA1, DG) and others are defined by their anatomic location along the long axis of the hippocampus (e.g. HEAD) – henceforth, we use the terms subfield and ROI interchangeably to refer to all of these subregions.

2.4 Statistical Analysis

Statistical analysis of activation within hippocampal ROIs followed an approach similar to Mueller et al. (2009) who studied structural atrophy within hippocampal subfields in unilateral TLE. Activation in 8 ROIs (HIPP, HEAD, BODY, TAIL, CA1, DG, CA3DG, CA) were considered as dependent variables that made up a multivariate observation vector and group membership (controls or patient) was considered as the independent variable. Activation in controls was averaged over the two hemispheres. Group effects were studied using a one-way multivariate analysis of variance (MANOVA) model. Two separate models were used for studying activation in patients' epileptogenic (ipsilateral to seizure focus) and non-epileptogenic (contralateral to seizure focus) hemispheres. Next, to compare the severity of disease effects relative to controls between different ROIs, activation A_S for each ROI was normalized to a z-score as

$$z(A_S) = \frac{A_S - \overline{A_S}^{controls}}{s_{A_S}^{controls}}$$

where $\overline{A_S}^{controls}$ and $s_{A_S}^{controls}$ represent mean and standard deviation of activation in subfield S over all control subjects respectively. These normalized z-scores were compared using one-way analysis of variance (ANOVA) with subfield as the independent variable to determine if subfields differed in their severity of disease effects. Again, epileptogenic and non-epileptogenic sides were analyzed separately. Normalized z-scores between pairs of subfields were also compared directly with each other in post-hoc analysis using Student's t-test.

Activation A_S between different groups (controls vs. epileptogenic, controls vs. non-epileptogenic, epileptogenic vs. non-epileptogenic, controls left vs. controls right) were also directly compared within each ROI using Student's t-test (Fig. 3).

In addition, we assessed whether DG had greater activation than CA1 within each of four groups of ROIs: control (left), control (right), patient (epileptogenic) and patient (non-epileptogenic). Functional dissociation of subfields has been demonstrated in healthy control subjects (Zeineh et al., 2003; Suthana et al., 2010; Duncan et al., 2011). In particular, subfields early in the hippocampal circuit such as DG and CA3 were found to be selectively active during episodic memory formation, whereas subfields later in the circuit such as subiculum and CA1 were more active during recollection (Eldridge et al., 2005). Therefore, we hypothesized that during our scene encoding task, DG will show greater activation than CA1. Note that we did not have a subiculum label in our study, but some part of the subiculum was included in the CA1 and HEAD labels. We tested this hypothesis by comparing activations A_{DG} and A_{CA1}, normalized by the respective subfield volumes, using Student's t-tests. We did not perform this type of analysis between all possible 28 pairs of subfields, since we did not have an a priori hypothesis about expected effects.

Finally, group difference in asymmetry index in each ROI between patients with left-sided and right-sided seizure foci was also assessed using Student's t-tests. AI within controls were tested for deviation from zero.

3 Results

3.1 Group analysis of functional activation within ROIs

Multivariate analysis of variance (MANOVA) using ROI activations as observations and group membership (controls vs. patients' epileptogenic side) as the independent variable revealed a significant group effect in the TLE-HR dataset (Wilks' lambda 0.49, $\chi^2(8)=22.92$, $p=0.005$). There was evidence for a group effect in the TLE-SR dataset, although it did not reach significance at $p<0.05$ level (Wilks' lambda 0.60, $\chi^2(8)=14.79$, $p=0.063$). This indicates that there are activation differences between the groups for some of the ROIs. In contrast, there was no significant group effect in patients' non-epileptogenic side in either dataset (TLE-HR: Wilks' lambda 0.74, $\chi^2(8) = 9.3$, $p=0.32$; TLE-SR:Wilks' lambda 0.64, $\chi^2(8)=12.97$, $p=0.11$); i.e., functional activation in the non-epileptogenic side of patients was not significantly different from controls.

To assess differences in disease effects between subfields, a comparison of the ROI activation z-scores normalized relative to controls was performed using a one-way ANOVA. A significant effect of "ROI" was found on the epileptogenic side (TLE-HR: $F(7,96)=2.64$, $p=0.01$, TLE-SR: $F(7,120)=2.73$, $p=0.01$), but not on the non-epileptogenic side (TLE-HR: $F(7,96)=0.40$, $p=0.89$, TLE-SR: $F(7,120)=1.09$, $p=0.37$). Post-hoc analysis was conducted comparing z-scores of certain pairs of subfields directly using Student's t-test. A significantly lower z-score in one ROI compared to another would indicate a greater disease effect. The TLE-HR dataset showed that in the epileptogenic hippocampi, at a coarse scale of subdivision, the HEAD ROI had a significantly lower z-score than BODY ($p=0.001$), TAIL ($p=0.002$), and whole hippocampus ($p=0.003$); and within the BODY, CA3DG had a significantly lower z-score than CA1 ($p=0.009$) and CA ($p=0.01$). In the TLE-SR dataset, the BODY ROI had a significantly lower z-score than HEAD ($p=0.0003$), TAIL ($p=0.047$), and whole hippocampus ($p=0.001$), and CA3DG again had the lowest z-score in the BODY, lower than CA1 ($p=0.009$) and CA ($p=0.04$).

Figure 3 plots all the activation data within each ROI for patients' epileptogenic and non-epileptogenic hippocampi, and controls' right and left hippocampi. Results of direct group

comparisons of activation in individual ROIs using Student's t-tests are shown. Connecting lines between pairs of bars with black stars indicate significant group difference at $p<0.05$ (uncorrected), and red stars indicate significance at a false discovery rate (FDR)-corrected (Yekutieli and Benjamini, 1999) threshold of $p<0.05$. All ROIs show lower activation in patients' epileptogenic side than the non-epileptogenic side, with the greatest effects in the hippocampus and HEAD among the larger ROIs, and in DG and CA3DG among the smaller ROIs in the body. Most ROIs also show lower activation in patients' epileptogenic side than controls (averaged over both sides). Controls' right TAIL had greater activation than the left side in TLE-HR, and patients' non-epileptogenic HEAD had greater activation than controls in TLE-SR.

3.2 Differential activation in hippocampal subfields within groups

We examined differences in functional activation between DG and CA1 subfields. Significantly greater activation in DG than in CA1 was found in controls in both sides. In contrast, in the epileptogenic side in patients, no evidence of differential activation between these two subfields was found, as shown in Fig. 4. In TLE-SR, there was no significant difference between DG and CA1 activation in either side of patients.

3.3 Functional Asymmetry Index within hippocampal ROIs

Asymmetry indices are commonly reported in studies of unilateral temporal lobe epilepsy (Jokeit et al., 2001; Golby et al., 2002; Deblaere et al., 2005), as it may have predictive power for clinical outcome. They were computed for all subjects within all 8 ROIs and are shown in boxplots in Fig. 5. AI in controls did not significantly differ from zero, indicating symmetric bilateral activation.

In patients, significant hippocampal activation asymmetry between epileptogenic and non-epileptogenic side was observed in the whole hippocampus, as well as within most subfields. AI for left and right TLE subjects were significantly different, with left TLE generally showing negative AI (right more active than left), and right TLE showing positive AI (left more active than right). In both datasets, dividing the hippocampus along its main axis showed the greatest effects in the HEAD region, whereas further subdividing the BODY region into subfields revealed the greatest effects in DG and CA3DG. CA1 subfield showed the least effect in both datasets.

4 Discussion

In this study, we applied a hippocampal subfield labeling method to BOLD fMRI acquired during a scene memory encoding task in TLE patients and controls. The study used shape-based normalization to a high resolution anatomical atlas of human hippocampus based on postmortem imaging to label the ROIs in *in vivo* anatomical scans. Consistent with existing findings, we found widespread inter-hemispheric activation asymmetry within the hippocampus as a whole as well as within several smaller ROIs in TLE patients, but not in controls (Section 3.3, Fig. 5). AI computed over the entire hippocampal ROI has previously been shown to help lateralize language and memory function in TLE patients (Binder et al., 2010; Rabin et al., 2004). In our data as well, hippocampal AI separates patients with left and right-sided disease. In addition, ROIs that showed the greatest separation in AI included the DG and HEAD (Fig. 5), which are among the regions known to be affected in TLE (Bernasconi et al., 2003; Sutula and Dudek, 2007; Mueller et al., 2009).

Activation was generally lower in all ROIs on the epileptogenic side in patients (Fig. 3), with strongest effects in HIPP, DG/CA3DG and HEAD, which is consistent with the AI analysis. In addition, activation in both hemispheres in controls was greater than on the

epileptogenic side in patients within several ROIs. Again, among the smaller ROIs in the BODY, this difference was most significant within the DG and CA3DG regions in both datasets, as also evident in posthoc analysis of normalized activation z-scores. In the TLE-HR dataset, this disease effect in HEAD is stronger than in the whole hippocampus. In the TLE-SR dataset, the effect is stronger in the entire BODY ROI than the whole hippocampus, and strongest in CA3DG. These results are concordant with subfield-specific hippocampal atrophy reported by Mueller et al. (2009), who found group effects in CA3DG in sclerotic hippocampi in TLE patients. They also agree with findings in previous structural studies that divided the hippocampus into approximate head, body, and tail regions and found greater atrophy in the HEAD region (Bernasconi et al., 2003). Note that the effects in the HEAD region may reflect underlying effects in the portion of DG subsumed into this ROI that wasn't labeled separately. Mueller et al. also found group effects of structural atrophy in CA1, which showed the least effect among ROIs in our data. This may be due to the specific task we used to activate the hippocampus (memory encoding), which is driven by DG, as shown previously (Zeineh et al., 2003; Eldridge et al., 2005; Suthana et al., 2010) – and more so than CA1, as we show in our CA1 vs. DG comparison (Fig. 4). In fact, a recent study by Mueller et al. (2011) found performance of TLE patients in memory encoding tasks to be correlated with atrophy in CA3DG, and that in recognition and recall tasks to be correlated with CA1 atrophy. Further, structural atrophy and functional activation effects may not always colocalize. Some researchers have also found greater right hippocampal activation in controls in scene encoding task (Powell et al., 2005). Our ROI analysis showed greater right hippocampal activation in the TAIL region, an effect that reached significance in the TLE-HR dataset. We previously found greater activation in the right posterior hippocampus of controls (Das et al., 2009), although that study used a different methodological approach. Interestingly, we found greater activation in the non-epileptogenic side of patients than in controls in the HEAD in the TLE-SR dataset – even though this effect was much weaker than inter-hemispheric activation asymmetry in patients. This may indicate compensatory mechanisms in the healthy hippocampi of patients. Similar effects have also been reported in the hippocampus in Alzheimer's disease (O'Brien et al., 2010).

Comparing activations between subfields, we found greater activation in DG than in CA1 in controls (Fig. 4), corrected for volume. Functional dissociation between hippocampal subfields is well known, and has been demonstrated in humans. In particular, DG has been shown to be selectively active during encoding (Zeineh et al., 2003; Eldridge et al., 2005; Suthana et al., 2010) in healthy controls, and might explain greater activation in DG than CA1 that we see during scene memory encoding task. However, this effect goes away in patients' epileptogenic hippocampi in our data, possibly due to pathology affecting activation in DG, consistent with what we see in group activation differences (Fig. 3) and inter-hemispheric activation asymmetry in patients (Fig. 5). This is further supported by a recent report (Mueller et al., 2011) that found memory encoding performance in TLE patients to be associated with atrophy in CA3DG.

4.1 Comparison of analyses of two datasets

The group effects of activation in the two independent datasets were broadly similar. There was a main effect of disease in the epileptogenic hippocampi, but not in the non-epileptogenic hippocampi. When comparing disease effects between ROIs, a main effect of ROI was present in both datasets. Post-hoc tests revealed greater disease effects in CA3DG than in CA1 in both datasets. Direct comparison of DG and CA1 activation within each group showed greater activation in DG in controls, but not in the epileptogenic hippocampi, in both datasets. The replication of these results in both datasets point to the robustness of these effects, and indicates that some subfield-specific effects can be observed even with 3 mm functional data, at least in larger ROIs.

It is also interesting to consider subtle differences in the results between the two datasets. In Fig. 3, significant difference in activation between patients' epileptogenic and non-epileptogenic side was present in all ROIs in TLE-SR, and the effect survived FDR-correction in all but one ROI (CA). In contrast, in the higher resolution TLE-HR dataset, this effect survived FDR correction only in the HEAD among the larger ROIs, and in DG and CA3DG among the smaller ROIs. CA1 did not show any group effect. This may be explained by the sensitivity vs. specificity tradeoff associated with spatial resolution of the data. In TLE-SR, the lower resolution – and thus, a larger smoothing effect – can provide greater sensitivity, thus resulting in stronger effects, but lacks spatial specificity due to mixing of signal between neighboring ROIs. In TLE-HR, the higher spatial resolution helps reveal the subfield-specific effects – in that DG shows a group effect, but the neighboring CA1 does not. Similar observations can be made about the post-hoc analysis with normalized activation z-scores where disease effects were compared between ROIs. CA3DG had greater disease effect than CA1 in both datasets, but had a stronger differential effect in the higher resolution TLE-HR dataset ($p=0.008$ vs. $p=0.016$). Also, the HEAD vs. TAIL comparison was only significant in the TLE-HR dataset. Even though these observations demonstrate the limitation of lower resolution data in detecting subfield-specific effects, there is still enough information present in the TLE-SR dataset such that the group effects – although present in all ROIs – are stronger in the DG, CA3DG and HEAD regions. This is illustrated in the group difference effects in activation (Fig. 3), as well as in the analysis of asymmetry index in Fig. 5. In addition, our processing of functional data in high-resolution anatomical space and lack of spatial smoothing may have helped retain some region-specific information in the data. Note that the TLE-SR and TLE-HR datasets also used slightly different versions of the memory encoding task (section 2), so we cannot rule out that some of the differences discussed above may be due to the difference in task. However, to establish this conclusively, one would need data from the same subjects at the same resolution but with two different tasks, and is beyond the scope of the current study.

4.2 Accuracy of shape-based labeling and localization of activation within sub-fields

Shape-based modeling of anatomical structures has been well-studied (Hogan et al., 2004; Yushkevich et al., 2006). It has been used in structural morphometry of the hippocampus in Alzheimer's disease (Csernansky et al., 2005; Thompson et al., 2004), epilepsy (Hogan et al., 2004), and other disorders (Wang et al., 2010). Shape analysis has proven to be particularly useful when intensity contrast in MRI images is insufficient to distinguish smaller anatomical substructures, such as hippocampal subfields, due to limited spatial resolution and partial volume effects. Even though higher resolution structural imaging can be used to accurately label hippocampal subfields (Mueller et al., 2008; Malykhin et al., 2010; Yushkevich et al., 2010), this may require special imaging sequences which are not widely available as part of a clinical examination protocol. In contrast, T1-weighted structural images with 1 mm isotropic resolution are widely available and routinely acquired in most clinical settings. While measurements of region volumes and structural changes are likely to be much more robust when there is enough intensity information available in the data in high resolution imaging, these relatively low contrast T1-weighted data have been used for functional analysis within hippocampal subfields, either using shape-based surface modeling (Wang et al., 2006) or using intensity-based normalization to a high resolution atlas (Miller et al., 2005). Therefore, we feel that our shape-based normalization approach, while not suitable for structural ROI analysis, nonetheless generates subfield labels that are accurate enough for ROI-based functional analysis, as evidenced by functional activation patterns found in this study that are consistent with existing literature. Also, our analysis method did not include any spatial smoothing of the functional data – unlike most neuroimaging studies – because we wanted to maximize our ability to localize activation

within small subregions. In addition, we resampled the functional data into the higher resolution anatomical space to help increase specificity (Kang et al., 2007).

4.3 Limitations and Future Work

One potential limitation of our work is the accuracy of subfield labels, as they are derived based on shape correspondence only, as discussed in section 4.2. We note, however, that accuracy of shape-based normalization has been evaluated in postmortem data (Yushkevich et al., 2008). To obtain more accurate subfield labels, we have begun collecting high resolution T2-weighted structural images, specifically designed to image the medial temporal lobe (MTL), which will likely improve the sensitivity of measurements. Labeling schemes based on these images can also be used to analyze activations in other MTL ROIs such as subiculum and entorhinal cortex (Mueller et al., 2008; Yushkevich et al., 2010). Also, the larger voxel sizes in functional data compared to structural ones limit the ability to localize activations within subfields, particularly for smaller ROIs such as CA2 and CA3, due to partial volume effects. Therefore, we did not analyze activation within these small ROIs, but included them in larger ROIs (CA2 is included in CA, CA3 is included in CA, as well as in CA3DG), similar to (Bakker et al., 2008; Suthana et al., 2010). This problem can be minimized by collecting fMRI data with even higher spatial resolution (Carr et al., 2010), which will also be part of our future work. Nonetheless, we believe that activation measures within larger subfields such as CA and DG are reliable with current spatial resolution.

Another limitation of this study is the small sample size of our clinical datasets. As such, these results should be treated as preliminary findings that need to be validated in a larger dataset. Nonetheless, focal measurements based on subfields have recently emerged as a valuable tool in studying both putative brain function and brain pathology in the hippocampus (Mueller and Weiner, 2009; Bakker et al., 2008). The potential value of the ability to perform this analysis in TLE has been recognized by other experts in the field (Richardson, 2010). We were able to demonstrate some results in the current dataset consistent with TLE literature. However, the clinical utility of these measurements can only be assessed by correlating them with clinical outcome variables such as post-surgical changes in cognitive ability (Rabin et al., 2004). We do not have this data for the TLE-HR dataset. We have some outcome data in the TLE-SR dataset, but the lower spatial resolution and small sample size will mean limited sensitivity for such analyses. We are currently expanding the TLE-HR dataset, and hope that future studies with a large enough sample size will allow us to conduct generalizable and meaningful studies of clinical correlations.

Finally, it is important to acknowledge that the sensitivity of all of the inter-hemispheric subfield-specific effects in patients, as well many of the cross-sectional effects in epileptogenic hippocampi of patients compared to controls in the current study are still lower than the effects in the whole hippocampus ROI, despite evidence of focal pathology from clinical non-imaging studies (Andrade-Valença et al., 2008; McAuliffe et al., 2011) and better sensitivity in structural imaging studies (Mueller et al., 2009). This again points to the limitation imposed by the sensitivity vs. specificity tradeoff with current image acquisition technology, as a larger ROI can offer better sensitivity, but loses the ability to detect more localized effects. Nonetheless, some disease effects (e.g. HEAD in TLE-HR, BODY and CA3DG in TLE-SR) were found to be stronger than whole hippocampus. One way to address this could be to extend the labeling scheme to the anterior (HEAD) and posterior (TAIL) hippocampus. In our data, the effect in the HEAD ROI is very strong, and within the BODY, DG and CA3DG have the strongest effects. Thus, it is possible that if DG was labeled fully along the length of the hippocampus, it could provide greater sensitivity than whole hippocampus. The extension of the labeling scheme is part of our ongoing work. As we mentioned earlier, the continued improvement of functional imaging and further increase in spatial resolution may also lead to more sensitive measurements in future.

Alternatively, it is possible that even though atrophy is localized, the effects on functional activation are sometimes relatively diffuse, and thus may not provide better sensitivity than whole hippocampus-based measurements.

5 Conclusion

In conclusion, we have presented a study of functional activation during an episodic memory task within intra-hippocampal ROIs in TLE that used a shape-based normalization technique to label subfield ROIs. We showed that activation differences exist within ROIs between subject groups and between hemispheres in patients, and between different subfields. Importantly, these group effects were stronger in certain ROIs than others – most notably in DG than in other regions within the BODY, and in HEAD than in BODY and TAIL, and sometimes stronger than in whole hippocampus. These results may indicate that functional measurements of disease effects in TLE can be specific to subregions of the hippocampus, and can potentially be used in combination with whole hippocampus based measurements to provide a richer characterization of the pathology.

Highlights

- We study functional activation patterns within hippocampal subfields during scene memory encoding in temporal lobe epilepsy.
- There are group differences in activation between controls and patients and between epileptogenic and non-epeileptogenic sides in patients.
- The disease effects vary in severity between subfields. Dentate gyrus (DG) and anterior hippocampus show the strongest effects.
- Encoding results in greater activity in DG than CA1 in controls, but not in patients' epileptogenic hippocampi.

Acknowledgments

This work was supported in part by the following grants: NIH R21 NS061111, NIH K25 AG02778, NIH K24 NS058386, NIH P30 NS045839, NIH T32 EB000814.

References

Andrade-Valença LPA, Valença MM, Velasco TR, Carlotti CG, Assirati JaA, Galvis-Alonso OY, Neder L, Cendes F, Leite JaP. Mesial temporal lobe epilepsy: clinical and neuropathologic findings of familial and sporadic forms. Epilepsia. 2008 Jun; 49(6):1046–1054. [PubMed: 18294201]

Bakker A, Kirwan CB, Miller M, Stark CEL. Pattern separation in the human hippocampal CA3 and dentate gyrus. Science. 2008 Mar; 319(5870):1640–1642. [PubMed: 18356518]

Bellgowan PS, Binder JR, Swanson SJ, Hammeke TA, Springer JA, Frost JA, Mueller WM, Morris GL. Side of seizure focus predicts left medial temporal lobe activation during verbal encoding. Neurology. 1998 Aug; 51(2):479–484. [PubMed: 9710022]

Bernasconi N, Bernasconi A, Caramanos Z, Antel SB, Andermann F, Arnold DL. Mesial temporal damage in temporal lobe epilepsy: a volumetric MRI study of the hippocampus, amygdala and parahippocampal region. Brain. 2003; 126(2):462. [PubMed: 12538412]

Bettus G, Guedj E, Joyeux F, Confort-Gouny S, Soulier E, Laguitton V, Cozzone PJ, Chauvel P, Ranjeva J-PP, Bartolomei F, Guye M. Decreased basal fmri functional connectivity in epileptogenic networks and contralateral compensatory mechanisms. Hum Brain Mapp. 2009 May; 30(5):1580–1591. [PubMed: 18661506]

Binder JR, Swanson SJ, Sabsevitz DS, Hammeke TA, Raghavan M, Mueller WM. A comparison of two fMRI methods for predicting verbal memory decline after left temporal lobectomy: language

lateralization versus hippocampal activation asymmetry. Epilepsia. 2010 Apr; 51(4):618–626. [PubMed: 19817807]

Bookheimer SY. Functional MRI applications in clinical epilepsy. Neuroimage. 1996 Dec; 4(3 Pt 3):S139–S146. [PubMed: 9345538]

Carr VA, Rissman J, Wagner AD. Imaging the human medial temporal lobe with high-resolution fMRI. Neuron. 2010 Feb; 65(3):298–308. [PubMed: 20159444]

Csernansky JG, Wang L, Swank J, Miller JP, Gado M, McKeel D, Miller MI, Morris JC. Preclinical detection of Alzheimer's disease: hippocampal shape and volume predict dementia onset in the elderly. Neuroimage. 2005 Apr; 25(3):783–792. [PubMed: 15808979]

Das SR, Mechanic-Hamilton D, Korczykowski M, Pluta J, Glynn S, Avants BB, Detre JA, Yushkevich PA. Structure specific analysis of the hippocampus in temporal lobe epilepsy. Hippocampus. 2009 Jun; 19(6):517–525. [PubMed: 19437496]

Deblaere K, Backes WH, Tieleman A, Vandemaele P, Defreyne L, Vonck K, Hofman P, Boon P, Vermeulen J, Wilmink J, Aldenkamp A, Boon PAJM, Vingerhoets G, Achten E. Lateralized anterior mesiotemporal lobe activation: semirandom functional MR imaging encoding paradigm in patients with temporal lobe epilepsy–initial experience. Radiology. 2005 Sep; 236(3):996–1003. [PubMed: 16118173]

Dice LR. Measures of the amount of ecologic association between species. Ecology. 1945; 26(3):297–302.

Duncan K, Ketz N, Inati SJ, Davachi L. Evidence for area ca1 as a match/mismatch detector: A high-resolution fmri study of the human hippocampus. Hippocampus. 2011 Apr.

Ekstrom AD, Bazih AJ, Suthana NA, Al-Hakim R, Ogura K, Zeineh M, Burggren AC, Bookheimer SY. Advances in high-resolution imaging and computational unfolding of the human hippocampus. Neuroimage. 2009 Aug; 47(1):42–49. [PubMed: 19303448]

Eldridge LL, Engel SA, Zeineh MM, Bookheimer SY, Knowlton BJ. A dissociation of encoding and retrieval processes in the human hippocampus. J Neurosci. 2005 Mar; 25(13):3280–3286. [PubMed: 15800182]

Engel, J. Surgery for seizures; New England Journal of Medicine. 1996 Mar. p. 647-653.URL http://dx.doi.org/10.1056/NEJM199603073341008

Figueiredo P, Santana I, Teixeira Ja, Cunha C, Machado E, Sales F, Almeida E, Castelo-Branco M. Adaptive visual memory reorganization in right medial temporal lobe epilepsy. Epilepsia. 2008 Apr.

Friston KJ, Glaser DE, Henson RNA, Kiebel S, Phillips C, Ashburner J. Classical and bayesian inference in neuroimaging: applications. Neuroimage. 2002 Jun; 16(2):484–512. [PubMed: 12030833]

Friston KJ, Holmes AP, Worsley KJ, Poline JB, Frith CD, Frackowiak RSJ, et al. Statistical parametric maps in functional imaging: a general linear approach. Human Brain Mapping. 1995; 2(4):189–210.

Golby AJ, Poldrack RA, Illes J, Chen D, Desmond JE, Gabrieli JDE. Memory lateralization in medial temporal lobe epilepsy assessed by functional MRI. Epilepsia. 2002 Aug; 43(8):855–863. [PubMed: 12181004]

Hogan RE, Wang L, Bertrand ME, Willmore LJ, Bucholz RD, Nassif AS, Csernansky JG. MRI-based high-dimensional hippocampal mapping in mesial temporal lobe epilepsy. Brain. 2004 Aug; 127(Pt 8):1731–1740. [PubMed: 15231583]

Huesgen CT, Burger PC, Crain BJ, Johnson GA. In vitro MR microscopy of the hippocampus in Alzheimer's disease. Neurology. 1993 Jan; 43(1):145–152. [PubMed: 8423879]

Jokeit H, Okujava M, Woermann FG. Memory fMRI lateralizes temporal lobe epilepsy. Neurology. 2001 Nov; 57(10):1786–1793. [PubMed: 11723264]

Kang X, Yund EW, Herron TJ, Woods DL. Improving the resolution of functional brain imaging: analyzing functional data in anatomical space. Magn Reson Imaging. 2007 Sep; 25(7):1070–1078. [PubMed: 17707169]

Killgore WD, Glosser G, Casasanto DJ, French JA, Alsop DC, Detre JA. Functional MRI and the Wada test provide complementary information for predicting post-operative seizure control. Seizure. 1999 Dec; 8(8):450–455. [PubMed: 10627406]

Kirwan CB, Jones CK, Miller MI, Stark CEL. High-resolution fMRI investigation of the medial temporal lobe. Hum Brain Mapp. 2007 Oct; 28(10):959–966. [PubMed: 17133381]

Lencz T, McCarthy G, Bronen RA, Scott TM, Inserni JA, Sass KJ, Novelly RA, Kim JH, Spencer DD. Quantitative magnetic resonance imaging in temporal lobe epilepsy: relationship to neuropathology and neuropsychological function. Ann Neurol. 1992 Jun; 31(6):629–637. [PubMed: 1514774]

Malykhin NV, Lebel RM, Coupland NJ, Wilman AH, Carter R. In vivo quantification of hippocampal subfields using 4.7 T fast spin echo imaging. Neuroimage. 2010 Jan; 49(2):1224–1230. [PubMed: 19786104]

McAuliffe JJ, Bronson SL, Hester MS, Murphy BL, Dahlquist-Topalá R, Richards DA, Danzer SC. Altered patterning of dentate granule cell mossy fiber inputs onto ca3 pyramidal cells in limbic epilepsy. Hippocampus. 2011 Jan; 21(1):93–107. [PubMed: 20014385]

Miller MI, Beg MF, Ceritoglu C, Stark C. Increasing the power of functional maps of the medial temporal lobe by using large deformation diffeomorphic metric mapping. Proceedings of the National Academy of Sciences. 2005; 102(27):9685.

Mueller SG, Laxer KD, Barakos J, Cheong I, Garcia P, Weiner MW. Subfield atrophy pattern in temporal lobe epilepsy with and without mesial sclerosis detected by high-resolution MRI at 4 Tesla: preliminary results. Epilepsia. 2009 Jun; 50(6):1474–1483. [PubMed: 19400880]

Mueller SG, Laxer KD, Scanlon C, Garcia P, McMullen WJ, Loring DW, Meador KJ, Weiner MW. Different structural correlates for verbal memory impairment in temporal lobe epilepsy with and without mesial temporal lobe sclerosis. Hum Brain Mapp. 2011 Mar.

Mueller SG, Schuff N, Raptentsetsang S, Elman J, Weiner MW. Selective effect of Apo e4 on CA3 and dentate in normal aging and Alzheimer's disease using high resolution MRI at 4 T. Neuroimage. 2008 Aug; 42(1):42–48. [PubMed: 18534867]

Mueller SG, Weiner MW. Selective effect of age, Apo e4, and Alzheimer's disease on hippocampal subfields. Hippocampus. 2009 Jun; 19(6):558–564. [PubMed: 19405132]

Nadel L, Moscovitch M. Memory consolidation, retrograde amnesia and the hippocampal complex. Curr Opin Neurobiol. 1997 Apr; 7(2):217–227. [PubMed: 9142752]

O'Brien JL, O'Keefe KM, LaViolette PS, DeLuca AN, Blacker D, Dickerson BC, Sperling RA. Longitudinal fMRI in elderly reveals loss of hippocampal activation with clinical decline. Neurology. 2010 Jun; 74(24):1969–1976. [PubMed: 20463288]

Pluta J, Avants BB, Glynn S, Awate S, Gee JC, Detre JA. Appearance and incomplete label matching for diffeomorphic template based hippocampus segmentation. Hippocampus. 2009 Jun; 19(6): 565–571. [PubMed: 19437413]

Powell HWR, Koepp MJ, Symms MR, Boulby PA, Salek-Haddadi A, Thompson PJ, Duncan JS, Richardson MP. Material-specific lateralization of memory encoding in the medial temporal lobe: blocked versus event-related design. Neuroimage. 2005 Aug; 27(1):231–239. [PubMed: 15927485]

Rabin ML, Narayan VM, Kimberg DY, Casasanto DJ, Glosser G, Tracy JI, French JA, Sperling MR, Detre JA. Functional MRI predicts post-surgical memory following temporal lobectomy. Brain. 2004 Oct; 127(Pt 10):2286–2298. [PubMed: 15329352]

Richardson M. Current themes in neuroimaging of epilepsy: brain networks, dynamic phenomena, and clinical relevance. Clin Neurophysiol. 2010 Aug; 121(8):1153–1175. [PubMed: 20185365]

Saravia FE, Beauquis J, Revsin Y, Homo-Delarche F, de Kloet ER, De Nicola AF. Hippocampal neuropathology of diabetes mellitus is relieved by estrogen treatment. Cell Mol Neurobiol. 2006; 26(4–6):943–957. [PubMed: 16807785]

Sass KJ, Lencz T, Westerveld M, Novelly RA, Spencer DD, Kim JH. The neural substrate of memory impairment demonstrated by the intracarotid amobarbital procedure. Arch Neurol. 1991 Jan; 48(1):48–52. [PubMed: 1986726]

Squire LR. Memory and the hippocampus: a synthesis from findings with rats, monkeys, and humans. Psychol Rev. 1992 Apr; 99(2):195–231. [PubMed: 1594723]

Stark CEL, Okado Y. Making memories without trying: Medial temporal lobe activity associated with incidental memory formation during recognition. Journal of Neuroscience. 2003; 23(17):6748. [PubMed: 12890767]

Sun H, Yushkevich PA, Zhang H, Cook PA, Duda JT, Simon TJ, Gee JC. Shape-based normalization of the corpus callosum for dti connectivity analysis. IEEE Trans Med Imaging. 2007 Sep; 26(9): 1166–1178. [PubMed: 17896590]

Suthana N, Ekstrom A, Moshirvaziri S, Knowlton B, Bookheimer S. Dissociations within human hippocampal subregions during encoding and retrieval of spatial information. Hippocampus. 2010 Sep.

Sutula TP, Dudek FE. Unmasking recurrent excitation generated by mossy fiber sprouting in the epileptic dentate gyrus: an emergent property of a complex system. Prog Brain Res. 2007; 163:541–563. [PubMed: 17765737]

Tabelow K, Polzehl J, Ulu AM, Dyke JP, Watts R, Heier LA, Voss HU. Accurate localization of brain activity in presurgical FMRI by structure adaptive smoothing. IEEE Trans Med Imaging. 2008 Apr; 27(4):531–537. [PubMed: 18390349]

Thompson PM, Hayashi KM, de Zubicaray GI, Janke AL, Rose SE, Semple J, Hong MS, Herman DH, Gravano D, Doddrell DM, et al. Mapping hippocampal and ventricular change in Alzheimer disease. Neuroimage. 2004; 22(4):1754–1766. [PubMed: 15275931]

Wang L, Miller JP, Gado MH, McKeel DW, Rothermich M, Miller MI, Morris JC, Csernansky JG. Abnormalities of hippocampal surface structure in very mild dementia of the Alzheimer type. Neuroimage. 2006 Mar; 30(1):52–60. [PubMed: 16243546]

Wang Z, Neylan TC, Mueller SG, Lenoci M, Truran D, Marmar CR, Weiner MW, Schuff N. Magnetic resonance imaging of hippocampal subfields in posttraumatic stress disorder. Arch Gen Psychiatry. 2010 Mar; 67(3):296–303. [PubMed: 20194830]

Yekutieli D, Benjamini Y. Resampling-based false discovery rate controlling multiple test procedures for correlated test statistics. Journal of Statistical Planning and Inference. 1999; 82(1–2):171–196.

Yushkevich PA, Avants BB, Pluta J, Das S, Minkoff D, Mechanic-Hamilton D, Glynn S, Pickup S, Liu W, Gee JC, Grossman M, Detre JA. A high-resolution computational atlas of the human hippocampus from postmortem magnetic resonance imaging at 9.4 T. Neuroimage. 2009 Jan; 44(2):385–398. [PubMed: 18840532]

Yushkevich PA, Avants BB, Pluta J, Minkoff D, Detre JA, Grossman M, Gee JC. Shape-based alignment of hippocampal subfields: evaluation in postmortem MRI. Med Image Comput Comput Assist Interv Int Conf Med Image Comput Comput Assist Interv. 2008; 11(Pt 1):510–517.

Yushkevich PA, Detre JA, Mechanic-Hamilton D, Fernández-Seara MA, Tang KZ, Hoang A, Korczykowski M, Zhang H, Gee JC. Hippocampus-specific fMRI group activation analysis using the continuous medial representation. Neuroimage. 2007 Feb; 35(4):1516–1530. [PubMed: 17383900]

Yushkevich PA, Wang H, Pluta J, Das SR, Craige C, Avants BB, Weiner MW, Mueller S. Nearly automatic segmentation of hippocampal subfields in in vivo focal T2-weighted MRI. Neuroimage. 2010 Jun.

Yushkevich PA, Zhang H, Gee JC. Continuous medial representation for anatomical structures. IEEE Trans Med Imaging. 2006 Dec; 25(12):1547–1564. [PubMed: 17167991]

Zeineh MM, Engel SA, Thompson PM, Bookheimer SY. Dynamics of the hippocampus during encoding and retrieval of face-name pairs. Science. 2003 Jan; 299(5606):577–580. [PubMed: 12543980]

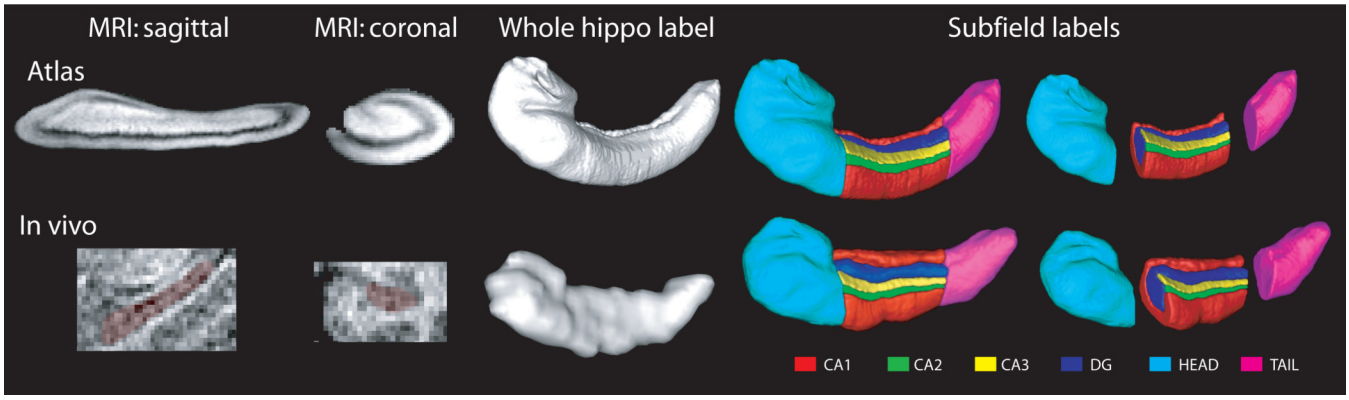

Fig. 1.
Postmortem atlas (top) and an example of normalization of an in vivo image (bottom). From left to right: sagittal MRI slice, coronal MRI slice, whole hippocampus label, subfield labels, and subfield labels with head, body and tail regions separately rendered to facilitate visualization of internal structures.

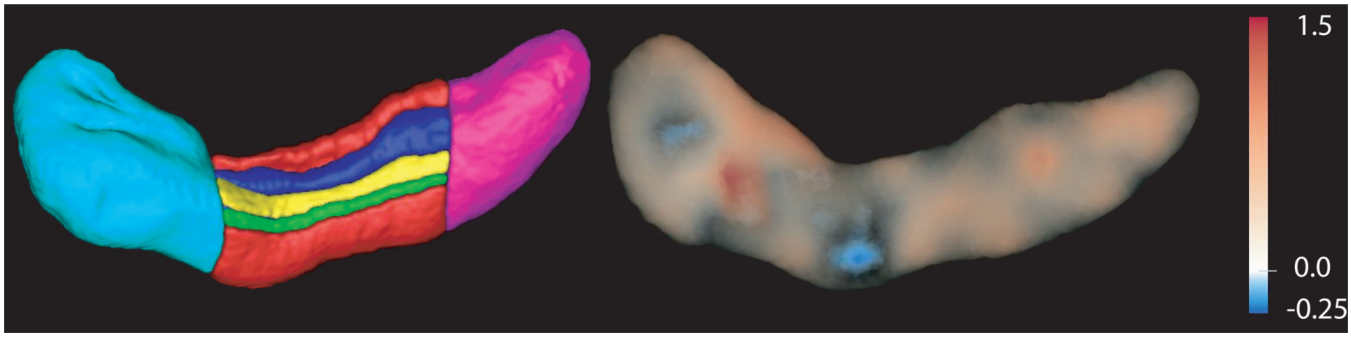

Fig. 2.
An example of subfield labels (left) and volume rendering of the task contrast map (right) in the hippocampus of a subject. Hotter colors indicate greater task-related activation.

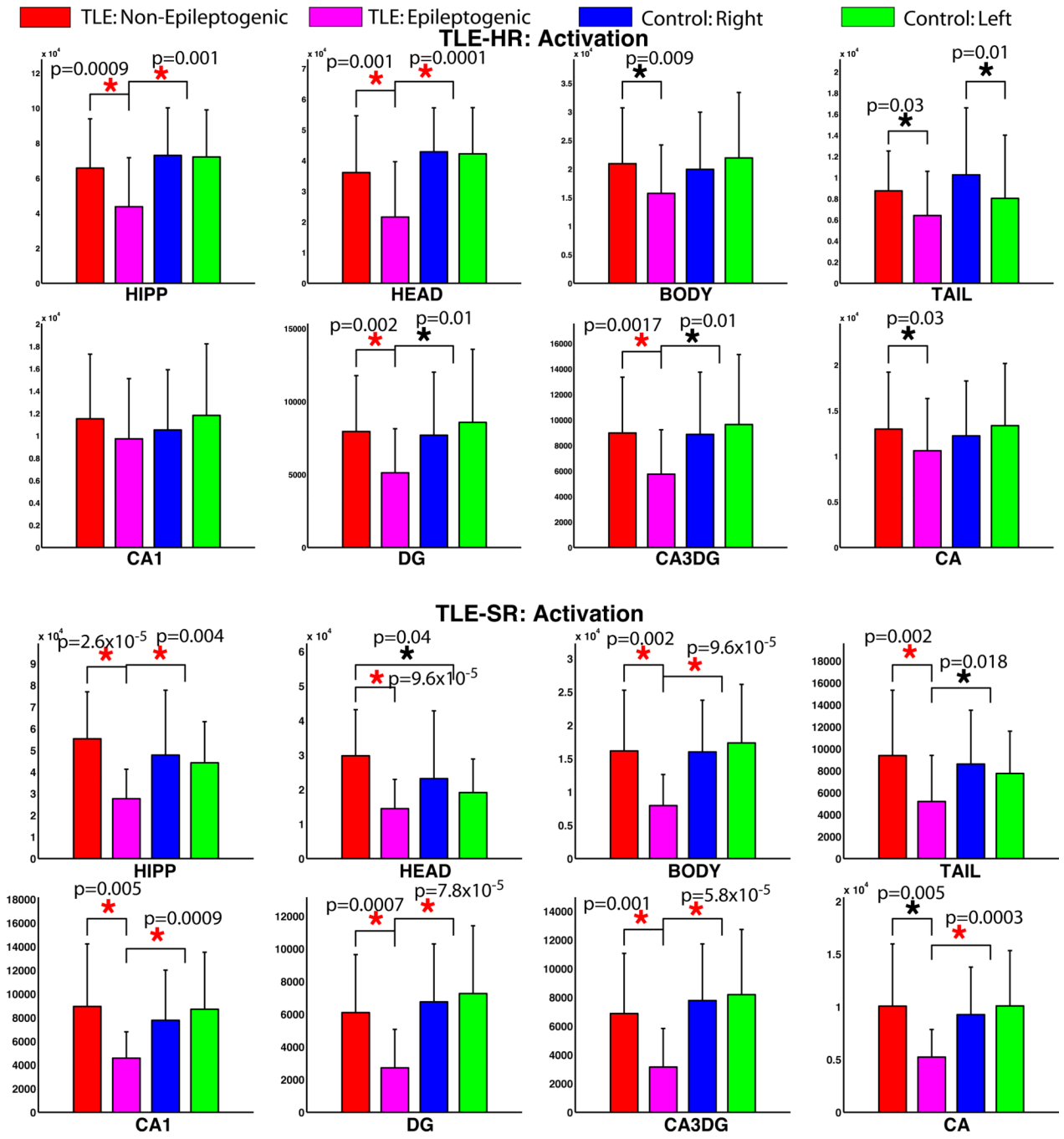

Fig. 3.

Group differences in activation within ROI: Activation is generally greater in non-epileptogenic (contralateral, red) side than epileptogenic (ipsilateral, magenta) side in patients, with largest effect in HIPP, DG and HEAD. Activations aren't significantly different between left (green) and right (blue) sides in controls, except in TAIL in the TLE-HR dataset. Lines connecting bars with stars on top indicate significant group difference ($p<0.05$ uncorrected) in activation between the two groups. Red stars denote the significant differences at an FDR-corrected threshold of $p<0.05$. p-values are shown in each case. Activation in controls is averaged over left and right sides for the purpose of comparing with patients' contralateral or ipsilateral sides.

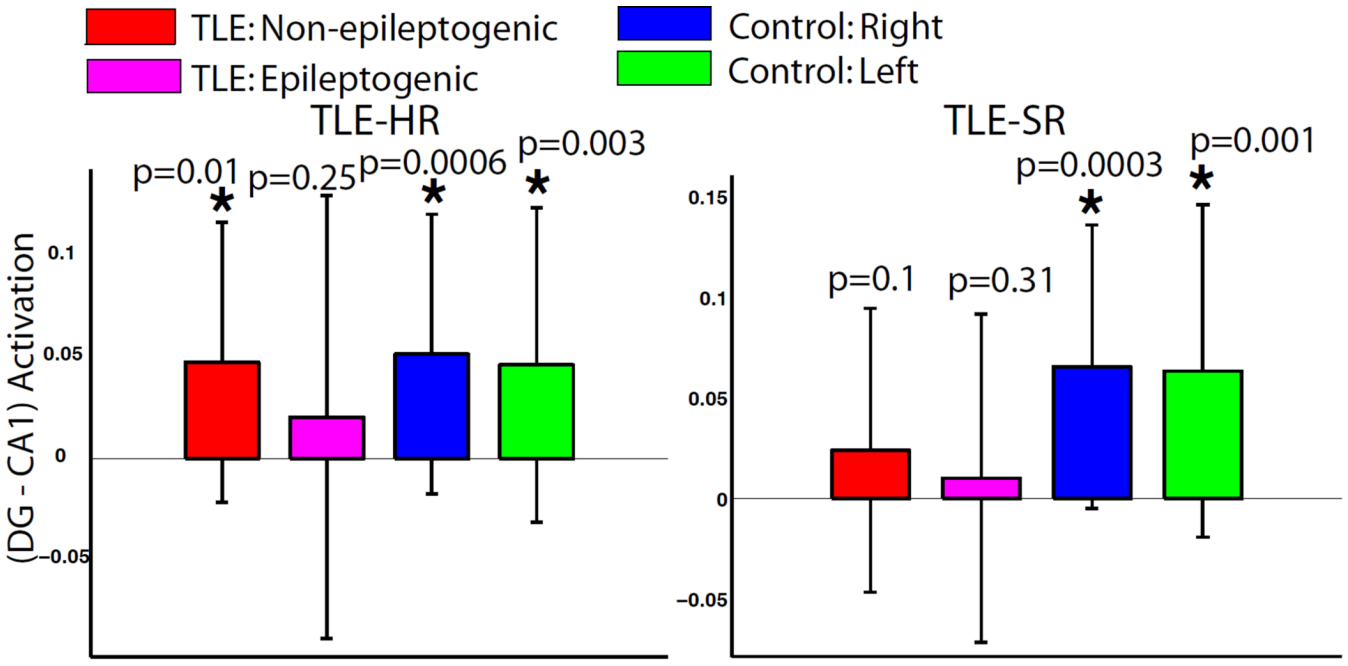

Fig. 4.

Within-group differences in functional activation between DG and CA1 subfields. DG has significantly greater activation in controls in both sides. There is no such significant group difference in activation between DG and CA1 in the epileptogenic side of patients in both datasets. Activations are normalized by the respective subfield volumes.

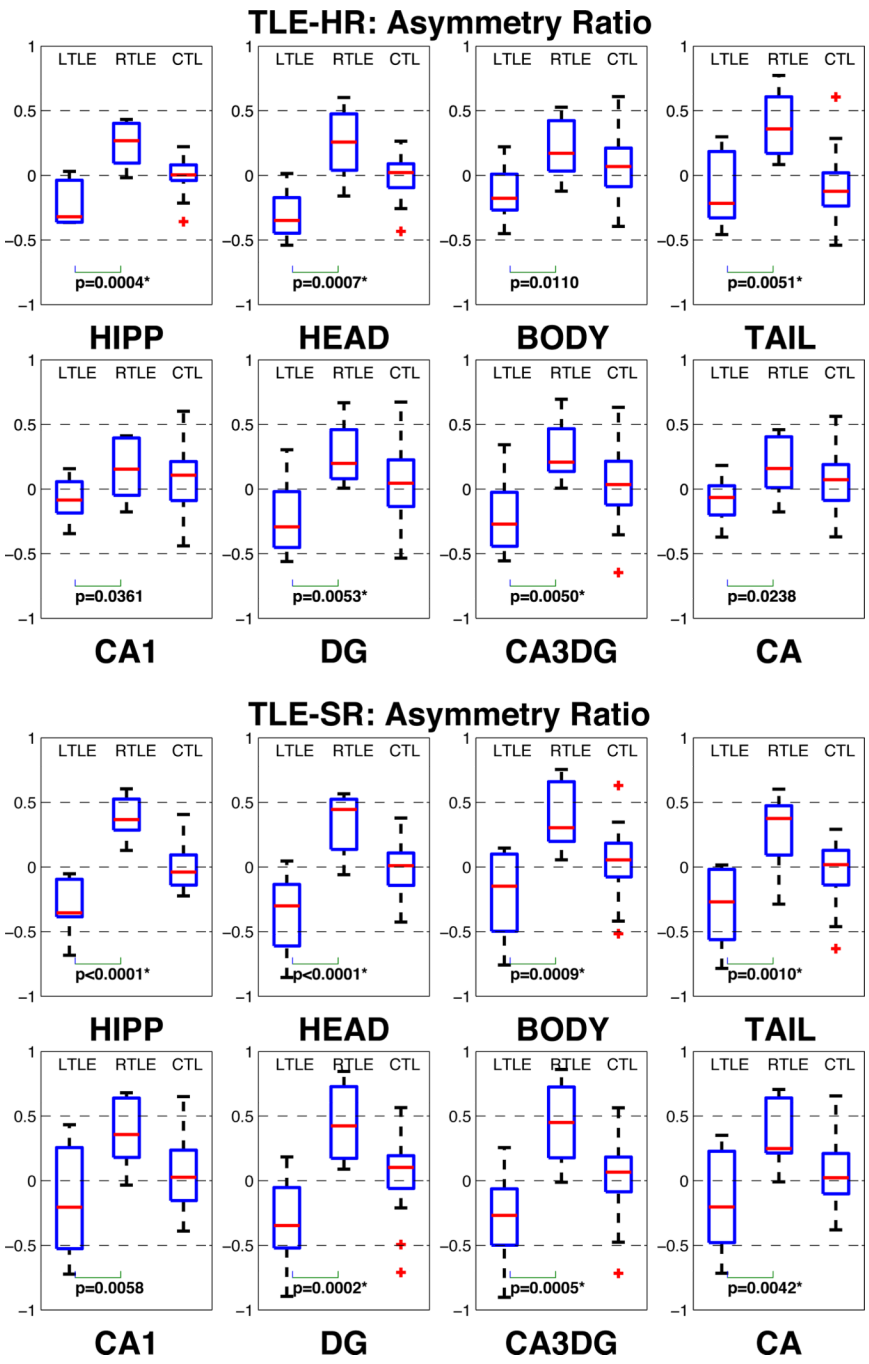

Fig. 5.

Boxplots showing activation asymmetry index within ROIs computed as (left − right)/(left + right). Data from TLE-HR and TLE-SR are shown separately. Each panel shows data from left TLE (LTLE) on the left, right TLE (RTLE) in the middle and controls (CTL) on the right. Patients show lateralization consistent with seizure side in the whole hippocampus, as well as several subfields, with the strongest effects in DG and HEAD. Controls do not show significant asymmetric activation within any ROI – AI isn't significantly different from zero in any subfield. *p*-values for significant separation of AI between LTLE and RTLE are indicated. "* " indicates those below the threshold at a false discovery rate (FDR) = 0.05.